Optical and Quantum Electronics **35:** 1025–1036, 2003.

High resonant reflection of a confined free space beam by a high contrast segmented waveguide

E. BONNET[1,*], X. LETARTRE[2], A. CACHARD[1], A. V. TISHCHENKO[1] AND O. PARRIAUX[2]
[1]*Laboratoire TSI UMR CNRS 5516, Université Jean Monnet, 10 Rue Barrouin, F-42000 Saint-Etienne, France*
[2]*LEOM, Ecole Centrale de Lyon, F-69031 Ecully, France*
*(*author for correspondence: E-mail: emmanuel.bonnet@univ-st-etienne.fr)*

Received 3 April 2003; accepted 1 May 2003

Abstract. High resonant reflection of a free space wave from a deeply corrugated slab waveguide is shown to take place in the case of a focused free space beam under normal incidence. It is described as a result of a strong intra-guide coupling coefficient allowing the coupled wave to be closely localized under the incident beam, therefore to interfere with it with high contrast effects. The coupled mode inspired analysis gives the possibility of optimizing the resonant structure; it is related and compared with the photonic crystal vision of the same functional structure to which it confers more intelligibility.

Key words: coupled modes, coupling gratings, diffraction gratings, photonic crystals, resonant reflection

1. Introduction

The electromagnetic problem of periodical structures of high index contrast is most often treated today from the standpoint of solid state physics with energy band concepts extrapolated to photons. A lot of efforts have been devoted to the numerical modelling of photonic band gap structures (PBG) with the objective of understanding them at the light of this new set of concepts. This drive is having a deep influence on the terminology of optical wave phenomena, and also on the way of seeing them. The aim of the present paper is to show how meaningful the coupled wave formalism remains, and to bridge it with the PBG vision in the case of a particular functional structure.

The functional structure which is considered here is a segmented waveguide of high index contrast and short period on which an incident focused free space beam impinges: the segmented waveguide is placed normally to the beam at the waist of the latter. The functional objective here is not to excite the segmented waveguide; it is to find out whether the presence of the deeply corrugated waveguide in the path of the focused beam does give rise to

narrow band resonant filtering effects such as 'abnormal reflection' as first discovered and analyzed by Golubenko *et al.* (1985) or 'resonant reflection' (Wang and Magnusson 1993) in the case of a plane free space wave impinging onto a infinite waveguide grating. If this were shown to be the case, much could be expected from this type of optogeometrical configuration such as narrow band polarizing mirror for VCSELs, monolithic refractive index sensors at the tip of a fibre, high density pixellated biosensor arrays of utmost sensitivity, high density matrices of detector filters, etc. However, even if one would not expect sharp diffraction effects on a beam which only 'sees' just a few grooves of a grating, high reflection gratings in PBG have been reported (Jakob *et al.* 2001). Shown here is what governs the properties of reflection effects in 1D deeply corrugated periodical structures from a waveguide mode standpoint. The present paper extends the vision of mode coupling to segmented waveguides of high contrast, and demonstrates numerically that narrow band reflection can be achieved on a focused beam 'seeing' only a restricted number of grating periods.

2. Abnormal reflection of a plane wave from a shallow waveguide grating

It is known (Avrutsky *et al.* 1986) that a polarized plane wave impinging onto an infinite slab grating waveguide experiences total reflection if the phase matching condition for the excitation of one of the waveguide modes of the same polarization is nearly satisfied through the plus or minus first diffraction order of the grating, and if there is no other diffraction order radiating the guided mode into the adjacent media. This reflection effect is wavelength and angularly dependent. It is vividly interpreted as shown in Fig. 1 as a result of the destructive interference in the transmitted medium between the plane wave transmitted through the waveguide grating by the zeroth order of the latter and the wave coupled into the slab waveguide, then re-radiated from the latter into the transmitted medium with a relative phaseshift of π. This phenomenon is resonant since the grating waveguide couples the energy of the incident plane wave and returns it to the adjacent media with a field amplitude and a phase which depend on the quality factor of the open resonator which the grating waveguide is, and on the degree of fulfilment of the mode excitation synchronism condition. The quality factor of the grating waveguide resonator is related to the field radiation coefficient α which is the rate of the leakage of the used modal field into the adjacent media due to the presence of the grating. A narrow band reflection filter (high quality factor) corresponds to a small value of α. $L_p = 1/\alpha$ defines a characteristic propagation length of the mode into the grating waveguide.

The same 100% reflection also takes place under normal incidence, and close to it. However, there are here two waveguide modes involved in the field

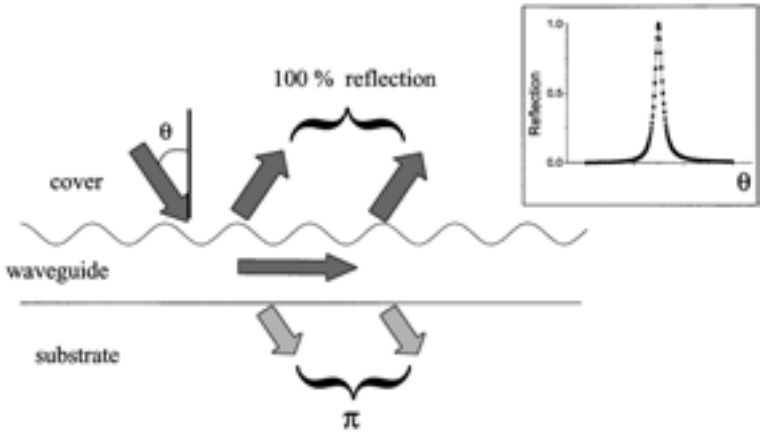

Fig. 1. Symbolic representation of abnormal reflection of a plane free space wave by a shallow waveguide grating. Destructive interference in the substrat causes 100% reflection. The insert shows a typical angular dependence of the reflection coefficient with zero background.

storage instead of single one: the +1st order forward coupled mode and the −1st order backward coupled mode. Then under strictly normal incidence, the wave trapped in the waveguide does not propagate any more: it has become a standing wave. A further effect is present which will play a very important role in deeply corrugated and segmented waveguides: the second order of the grating couples the forward to the backward propagating mode through the intra-guide coupling coefficient κ. From a phenomenological point of view, this intra-guide coupling tends to shorten the propagation length of the modes in the waveguide since, in addition to leaking into the adjacent media at the rate α, each mode experiences a distributed reflection over a length of the order of $2\pi/\kappa$ which can be lower than L_p. Intra-guide coupling does not alter the spectral line width of the resonant reflection since it keeps the guided field in the waveguide; the waveguide resonator is not more open than under non-normal incidence; α does not change significantly. This effect of κ remains somewhat hidden in the case of plane wave excitation, but it will become dramatic in the case of confined beam excitation as described in Section 3.2.

3. Reflection on a high contrast segmented waveguide

3.1. PLANE WAVE CASE

Leaving aside for a while the above phenomenological approach of wave coupling, the problem of the diffraction of a plane wave by a large contrast

segmented layer was submitted to the exact method of generalized sources (Tishchenko 2000). The objective was to identify the conditions for mode excitation and for a maximum reflection (possibly 100%).

In a first step, the structure parameters were chosen so as to roughly correspond to the excitation of a guided mode of the segmented waveguide in the vicinity of $\lambda = 1.55$ μm. To that end, equivalent index reasoning was used although this representation is only valid when the segmentation period is much smaller than the wavelength. This nevertheless provides some guidance to choose optogeometrical parameter values in order to anticipate the waveguide resonance wavelength. Then the generalized source method is used for the exact calculations and the fine adjustment of the parameters. As illustrated as an example in Fig. 2, 100% abnormal reflection was found under normal incidence for a structure characterized by a silicon segmented waveguide of index $n_g = 3.47$, period $\Lambda = 0.870$ μm, line/space ratio of 0.428 (filling factor $f = 0.3$), layer height $h = 590$ nm, and substrate and cover index $n_s = 1.45$ and $n_c = 1.45$ respectively. Fig. 2 exhibits a narrow spectral linewidth of 0.01 nm at $\lambda_R = 1.55792$ μm, which can be varied by small variations of the optogeometrical parameters. This example is only illustrative: as a matter of fact, 100% reflection can be obtained with plane waves whatever the structure parameters as long as the spatial frequency of the waveguide segmentation does not give rise to propagating diffraction waves of orders different from 0, +1 and −1. This is not the case with a confined beam as discussed in the next section.

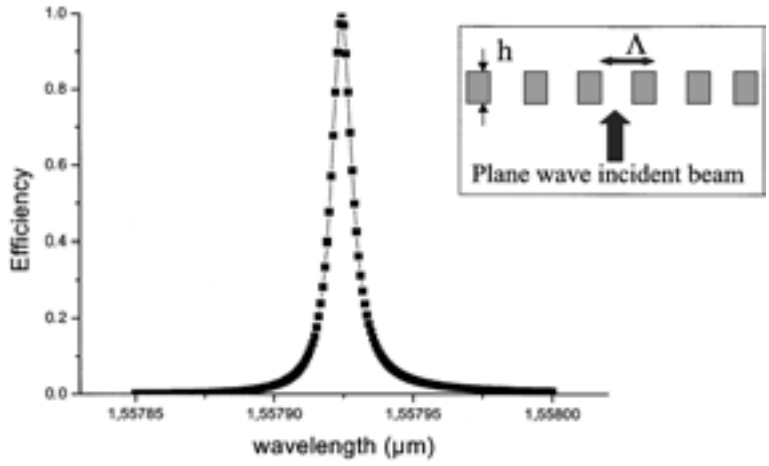

Fig. 2. Narrow spectral linewidth abnormal reflection from a segmented silicon waveguide embedded in SiO_2 for a TE plane wave under normal incidence. $h = 590$ nm, $\Lambda = 0.870$ μm, $f = 0.3$, $n_g = 3.47$, $n_s = n_c = 1.45$, $\lambda_R = 1.55792$ μm, $\delta_{1/2} = 8$ pm.

3.2. CONFINED BEAM CASE

Exact numerical modelling as performed above did not give a hint as to what should the parameters be to give rise to narrow band reflection, and no guarantee that 100% reflection would be preserved in case of confined beam incidence. The structures exhibiting 100% reflection under plane wave incidence was submitted to a 2D FDTD code. The confined incident beam of TE polarization was the fundamental mode of a 6 μm width symmetric waveguide. The waveguide index was 1.45 and the adjacent media index was 1.44, giving a mode width of 9 μm. As compared with the plane wave modelling, first examples treated by the FDTD exhibited a catastrophic fall of the reflection coefficient (Fig. 3). However, a small reflection was still where it was expected to be (within a shift of 2 nm). Our interpretation of what happens is illustrated schematically in Fig. 4 where it is shown that the field trapped in the segmented waveguide propagates a long way outside the region illuminated by the confined incident beam. This leads to a fall of the reflection since the energy coupled in the waveguide propagates away and leaks into the adjacent media outside the impact zone of the incident beam where it cannot interfere any more with the latter. Fig. 5 represents the field in the segmented waveguide at the resonance peak of Fig. 3; it confirms the interpretation that the guided field extends far outside the impact zone of the incoming beam. Figs. 4 and 5 suggest that for the trapped wave to interfere with the incoming, reflected and transmitted beams, the former must be laterally confined within

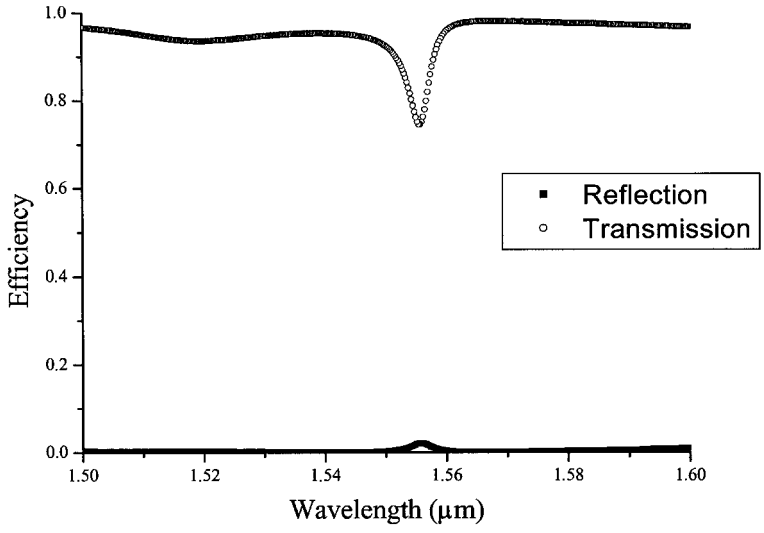

Fig. 3. Reflection of the same segmented silicon waveguide structure as for Fig. 2 with a focused beam. The focused beam was represented by the fundamental mode of a symmetric waveguide with 6 μm width and 1.45 index, the adjacent media index being 1.44.

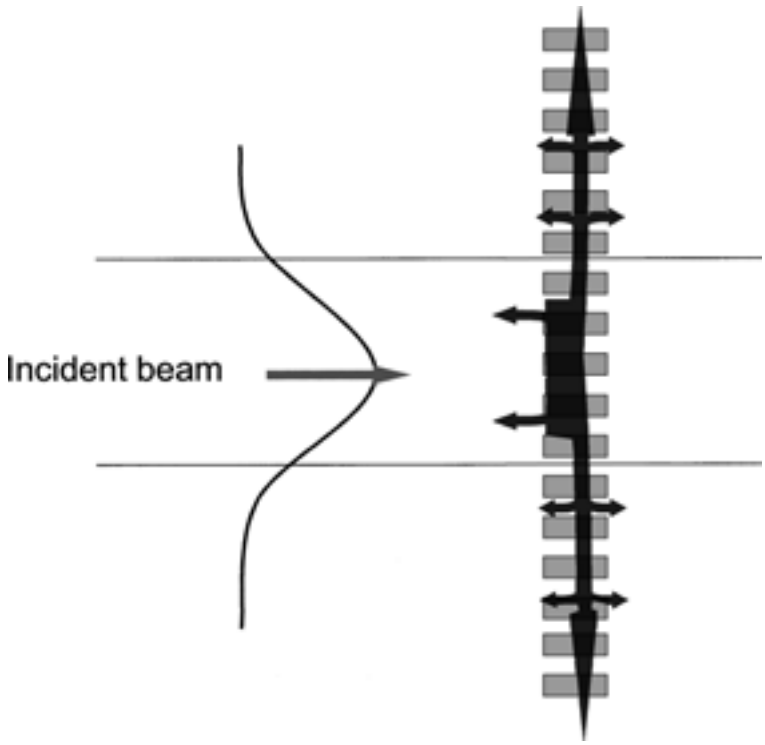

Fig. 4. Symbolic representation of the leak of the coupled guided wave propagating away from the impact zone of the normal incident wave in case of weak intra-guide coupling coefficient.

a segmented waveguide section having a length comparable with the cross-section of the latter. This confinement can be achieved by creating a resonant cavity in the segmented guide or by intra-guide distributed reflection via the second order intra-guide coupling coefficient κ according to a coupled mode representation. This is this second effect that we want to exploit which calls for an increase of κ.

4. The search for a large intra-guide coupling coefficient κ

We have determined the second order coupling coefficient κ between the forward and the backward modes of same order in a high contrast segmented waveguide by means of the numerical experiment of the virtual prism (Pigeon *et al*. 2002) as illustrated in Fig. 6. The model used is the following.

The incident beam impinges onto the basis of a prism of high index n_p under an angle θ larger than the critical angle similarly to the well known '*m*-lines' measurement technique by means of a high index prism. The segmented

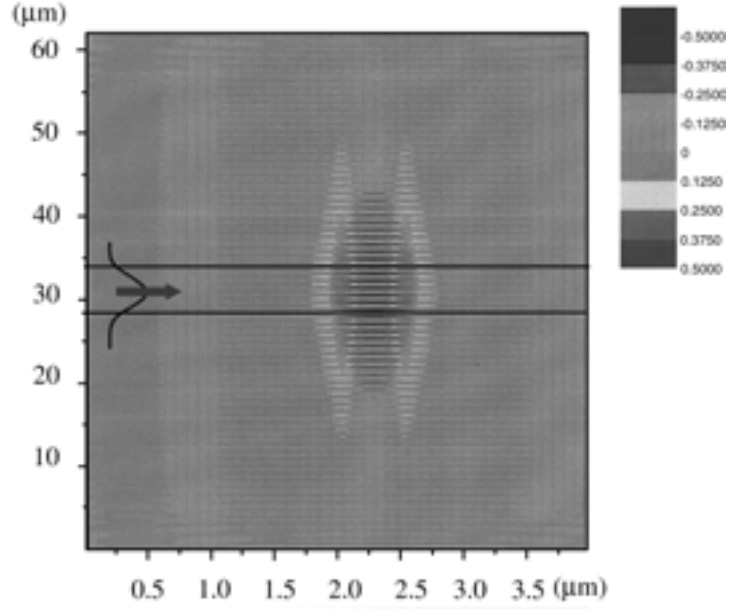

Fig. 5. FDTD modelling of the electric field at resonance for the segmented silicon waveguide structure of Fig. 3.

waveguide excitation is achieved via the evanescent wave. The wavelength λ, the waveguide thickness w and the duty cycle of the waveguide period are kept constant. The numerical experiment consists in scanning the incident angle θ for finding out the waveguide mode resonances for each value of the period Λ. The resonances are identified as a dip in the reflection coefficient at the basis of the prism. The abcissa of the graph of Fig. 7 is the projection of the incident k-vector in the prism on the propagation direction: $k_0 n_p \sin\theta$. Starting with large grating periods, there are two angles, θ_1 and θ_2, for each K_g value ($K_g = 2\pi/\Lambda$) at which the mode is excited as suggested in Fig. 6: the incidence angle θ_1 corresponds to the usual prism forward excitation with the phase matching condition $k_0 n_p \sin\theta_1 = \beta$ where β is the real part of the modal propagation constant, whereas θ_2 corresponds to the backward excitation condition by means of diffraction order m of the grating characterized by the synchronism condition $k_0 n_p \sin\theta_2 = mK_g - \beta$. In the present case intra-guide coupling involves the second grating order, $m = 2$. If the two contra-propagating modes were not coupled, increasing K_g (the ordinate of the graph of Fig. 7) would lead to two lines crossing each other at $K_g = \beta$: one quasi-straight line close to vertical with large negative slope corresponding to the forward mode excited by frustrated total reflection (the effective index is a slightly increasing function of the period Λ), and one oblique quasi-straight line of positive slope corresponding to the grating excited backward

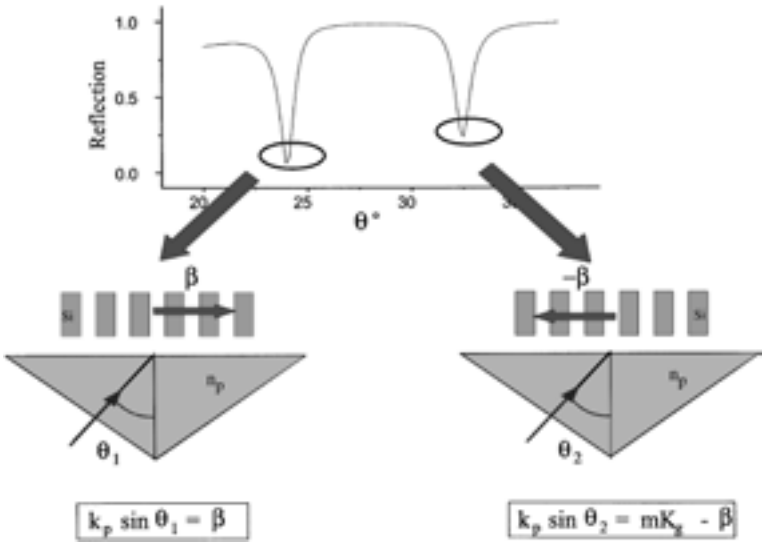

Fig. 6. Sketch of the virtual excitation prism experiment whereby the guide mode is excited in the forward direction by frustrated total reflection and in the backward direction by – second order grating coupling.

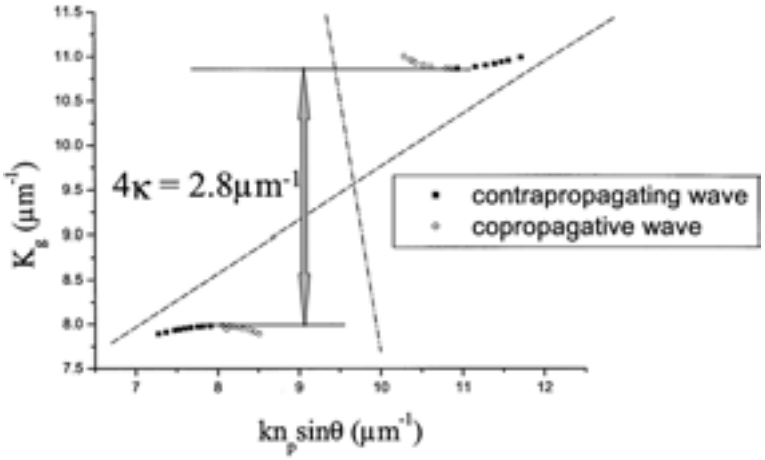

Fig. 7. Mode excitation curves in the spatial frequency plane ($k_0 n_p \sin\theta$, K_g) in a Si/SiO_2 segmented structure of 546 nm thickness, 0.52 fill factor, excited by a plane wave at 1.5497 μm wavelength experiment. The gap width 4κ is 2.8 μm^{-1}.

propagating mode. But the contra-propagating modes get increasingly coupled by the second order of the grating as K_g gets close to β. As illustrated in Fig. 7, this coupling opens a gap in the K_g space where no mode can be excited. The coupled wave analysis in the mechanism of free space wave waveguide grating coupling (Pigeon *et al.* 2002) teaches that the width of the

gap along K_g is equal to 4κ where κ stands for the modulus of the intra-guide coupling coefficient. This important property gives access to the intra-guide coupling coefficient which is responsible for the limitation of the propagation length of the guided modes when excited under normal incidence. Therefore this is the key for increasing κ so as to reduce the distributed reflection length $2\pi/\kappa$ down to the width of the incoming beam. That the width of the gap is 4κ is stated under the assumption that the theory of coupled waves is applicable to the segmented waveguide of high contrast. This is debatable and will be clarified in another article. However, the numerical results obtained tend to confirm the plausibility of this assumption. The structure used in Fig. 2 was submitted to the virtual prism experiment. It was found that the coupling coefficient is as small as 0.125 μm^{-1} giving rise to an interaction length of 50 μm which is consistent with the field extent shown in Fig. 5. This indicates that the coupled field escapes far outside the impact zone of a 9 μm width incident mode and cannot interfere with the latter, giving rise to a dramatic decrease in the reflection coefficient.

The search for the structure exhibiting a large κ value (large confinement factor) was undertaken systematically. In the case of segmented silicon waveguide imbedded in SiO_2 ($n_{Si} = 3.47$, $n_{SiO_2} = 1.45$ at 1.55 μm wavelength) a number of structures have been identified. We obtained maximum values of κ of the order of 0.7 μm^{-1} for a nearly 1 line/space ratio (filling factor in the 0.45/0.55 range), a period Λ in the 750/850 nm range and a thickness w in the 550/600 nm range. Fig. 7 is an illustration of such results for specific parameter values. The associated distributed reflection length is then of 9 μm, that is of the order of the incident beam width.

Figs. 8 and 9 are obtained by FDTD with a segmented silicon waveguide imbedded in SiO_2 with the following parameter values: $\Lambda = 800$ nm period, 1 line/space ratio (filling factor of 0.5) and $w = 550$ nm thickness. The confined incident beam was represented by the same fundamental mode of a symmetric waveguide used in Section 3.2. Fig. 8 shows that the guided field at resonance has the same symmetry as in Fig. 5 but it now remains confined under the incident beam which translates in the spectral response of Fig. 9 showing a spectacular increase of the resonant reflection, larger than 85%, and zero transmission as compared with the small reflection peak of the structure of Fig. 3. It has been systematically verified that the field confinement and related reflection properties are independent of the width of the FDTD calculation window and of the possible presence of an index discontinuity next to the confinement section in the segmented waveguide. Besides, the field confinement and related high reflection properties have been independently confirmed by Photon Design by means of the fundamentally different modelling approach of an eigenmode expansion technique.

Interesting also is the fact that the spectral linewidth of the resonance peak given by the FDTD remains quite narrow (<2 nm), even though it is 1 or 2

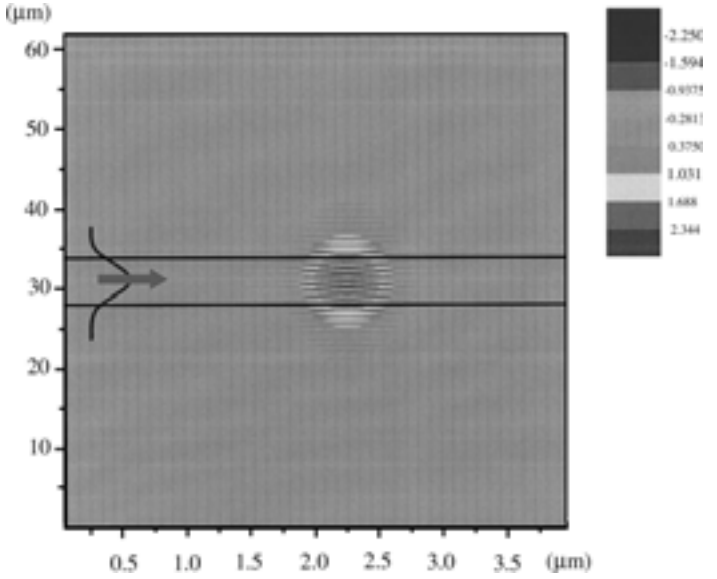

Fig. 8. FDTD modelling of the electric field at resonance for a Si/SiO_2 segmented waveguide of 550 nm thickness, 0.5 fill factor and 800 nm period, excited at normal incidence by the same focused beam as Fig. 3.

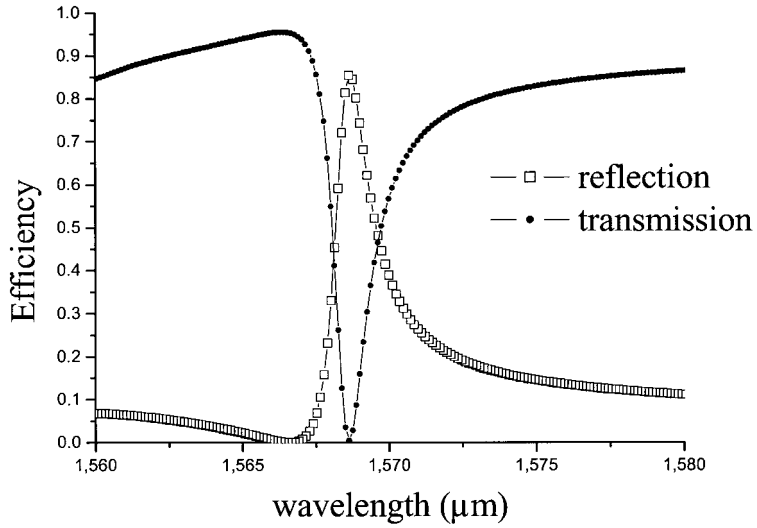

Fig. 9. Spectral response corresponding to, the structure of Fig. 8. $\lambda_R = 1.56863$ μm, $\delta_{1/2} = 1.4$ nm.

order of magnitude larger than that given by the plane wave approach. Also observed is a shift of the resonance wavelength obtained by FDTD (up to 15 nm) relative to the spectral location of the plane wave resonance. The eigenmode expansion technique gives a peak location and a spectral width

which are significantly closer to that given by the plane wave approach. The cause of these two discrepancies is presently under study and will be the subject of a joint publication.

5. The dispersion curve and the photonic crystal interpretation

The virtual prism experiment has been performed again at constant segmentation period Λ and variable wavelength λ. The diagram of Fig. 10 represents a typical dispersion curve ($1/\lambda$, versus $k_0 n_p \sin\theta$) obtained with the same structure as in Fig. 7, the period being $\Lambda = 0.785$ μm and the wavelength range in the vicinity of the resonance. As expected, this graph exhibits a gap in the optical frequency domain. A number of such graphs have been calculated and compared with those of K_g versus $k_0 n_p \sin\theta$. The comparison shows that a large second order coupling coefficient κ corresponds to a large photonic band gap. It is not possible at this stage to state that there is a strict proportionality between κ and the gap width. The larger resonant reflection is shown to be close to the high energy band edge of the photonic crystal waveguide where the dispersion curve flattens and the group velocity tends to zero (the guided field is close to a standing wave). The obtained results compare qualitatively well with those of Bendickson *et al.* (2001).

6. Conclusion

The effect of large resonant reflection is shown to take place on high contrast segmented waveguides for incident beams of essentially normal incidence

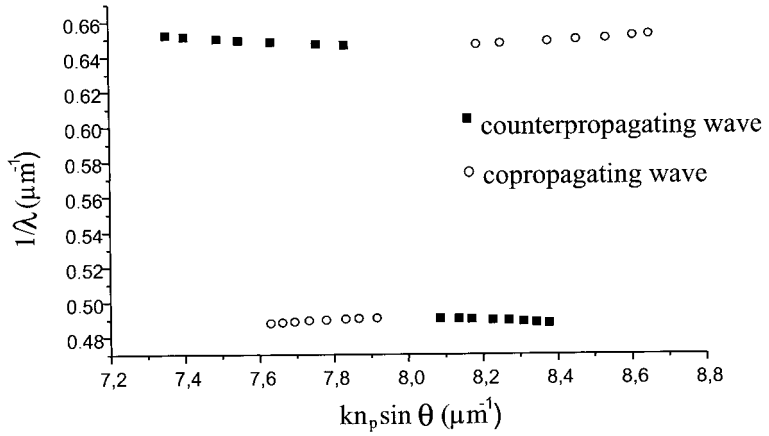

Fig. 10. Dispersion curve ($1/\lambda$ versus $k_0 n_p \sin\theta$) in the optimized structure of Fig. 7.

cylindrically focused on the waveguide. This effect which can be narrow line is shown to be governed by the second order intra-guide coupling coefficient κ between the contra-propagating modes of the segmented guide. A method is disclosed which allows the design of structures exhibiting a large coupling coefficient giving a confinement zone equal to the cross-section of the incident beam.

It is shown that the condition of high abnormal reflection also corresponds to a segmented structure which operates close to the second band edge of the photonic crystal represented by the periodically segmented high index layer, and that the second order intra-guide coupling coefficient κ and the width of the photonic band gap vary in the same way upon a change of the fill factor.

Further work is required to identify the modal field in high contrast segmented waveguides and to reformulate the coupled wave mechanism.

An outcome of the present analysis is an enrichment of the intelligibility and of the design possibilities of high contrast periodic optical structures thanks to a coupled wave inspired vision.

Acknowledgements

The Rhône–Alpes Region is gratefully acknowledged for supporting this work under project. The authors want to thanks Dr P. Viktorovitch and team (LEOM, Ecole Centrale de Lyon) for numerous enlightening discussions. They are very grateful to Dominic Gallagher, Photon Design, for checking our results by means of the eigenmode expansion technique and for his useful contribution to the understanding of the structure behaviour.

References

Avrutsky, I.A., G.A. Golubenko, V.A. Sychugov and A.V. Tishchenko. *Sov. J. Quant. Electr.* **16** 1063, 1986.

Bendickson, J.M., E.N. Glytsis, T. Gaylord and D.L. Brundrett. *J. Opt. Soc. Am. A* **18** 1912, 2001.

Golubenko, G.A., A.S. Svakhin, V.A. Sychugov and A.V. Tishchenko. *Sov. J. Quant. Electr.* **16** 886, 1985.

Jakob, D.K., S.C. Dunn and M.G. Moharam. *J. Opt. Soc. Am. A* **18** 2109, 2001.

Pigeon, F. and A.V. Tishchenko. *Opt. Quant. Electr.* **34** 505, 2002.

Tishchenko, A.V. *Opt. Quant. Electr.* **32** 971, 2000.

Tishchenko, A.V., M. Hamdoun and O. Parriaux. *Opt. Quant. Electr.* this issue.

Wang, S.S. and R. Magnusson. *Appl. Opt.* **32** 2606, 1993.